The effect of plastic anisotropy on the calibration of an equivalent model for clinched connections

Andreas Breda[a], Sam Coppieters[a], Toshihiko Kuwabara[b], Dimitri Debruyne[a]

[a] *Department of Materials Engineering, KU Leuven (Technology Campus Ghent), Gebroeders De Smetstraat 1, Ghent 9000, Belgium*
[b] *Division of Advanced Mechanical Systems Engineering, Tokyo University of Agriculture and Technology, 2-24-16 Nakacho, Koganei-shi, Tokyo 184-8588, Japan*

Abstract

To increase the accuracy of an equivalent clinch joint model, the effect of plastic anisotropy and residual material state is investigated by using three different yield functions (von Mises, Hill's 48 and Yld2000-2d). The results show that the residual stress state affects the calibration accuracy of the elastic and plastic parameters of the equivalent model in the normal direction of the joint. Moreover, it is shown that the adopted yield function significantly affects the calibration of the plastic model parameters. For the shear direction of the joint, however, the choice of the yield function does not affect the calibration accuracy.

Keywords: Clinching, Equivalent FE modelling, Simplified Elements, Joining, Material Anisotropy

1. Introduction

In recent years, lightweight constructions have gained more interest. In this perspective, the need to join dissimilar, coated or hard to weld lightweight materials, led to the rapid development of mechanical joining techniques such as rivets, self piercing rivets (SPR) and clinched joints. In the field of construction, automotive, heating ventilation and air conditioning (HVAC), multiple (dissimilar) joints are used in order to obtain the desired design features within different

Email addresses: andreas.breda@kuleuven.be (Andreas Breda), sam.coppieters@kuleuven.be (Sam Coppieters), kuwabara@cc.tuat.ac.jp (Toshihiko Kuwabara), dimitri.debruyne@kuleuven.be (Dimitri Debruyne)

regions of the constructions. To numerically predict the mechanical behaviour of these constructions, an accurate response of the joint is needed. In a numerical analysis, it is not computationally feasible to include detailed sub-models of these joints. Therefore, depending on the application, several equivalent or simplified models were developed which can be applied to predict the mechanical behaviour under different static, or dynamic load conditions. Langrand et al. [1] proposed a simplified element to simulate rivet joint behaviour for airframe crash worthiness. The equivalent model was validated using a structure containing 700 riveted joints. The accuracy of the element, however, further needed to be improved as the global stiffness and failure mode could not be accurately described. The multi-axial behaviour of the equivalent model in this work was calibrated using the experimental results of the modified Arcan test. The latter was initially proposed by Porcaro et al. [2] proposed the modified Arcan test in order to obtain the multi-axial behaviour of self piercing riveted (SPR) joints. This device allowed the user to control the tensile/shear ratio of a joint during a tensile test and is proven beneficial to investigate multi-axial joint behaviour. Coppieters et al. [3] used the device to investigate the behaviour of clinched joints under multi-axial loads. It was found that friction conditions and post-necking work hardening behaviour of the sheet metal are of major importance to numerically predict the deformation behaviour under mixed mode loads. However, the study was limited to steel sheet with identical thickness. For future work, multi-axial behaviour of dissimilar clinched joints with different thickness should be further investigated. For spot welds, simplified models were developed for static and dynamic analysis. Xu et al. [4] evaluated the performance of several equivalent models for spot welds. The investigated spot-weld models could accurately reproduce the stiffness behaviour when subjected to certain load conditions (tension, out-of-plane torsion and out-of-plane bending). However, there is still room for improving the predictive accuracy for in-plane torsion and in-plane shear. Khandoker et al. [5] used a H-tension test to validate six simplified spot weld models and concluded that the spider models *SC-2* and *SC-3* were preferable for static stress and dynamic

crash analysis in terms of computational cost and accuracy. Palmonella et al. [6] gave an overview of spot weld equivalent models were the model accuracy is updated using a finite element algorithm. This is validated using a single- and double hat benchmark experiment. The conclusion shows that the single beam elements are inaccurate compared to the more complex models due to the limited updating possibilities. Hanssen et al. [7] developed a point-connector model for large scale crash simulations with SPR joints. The results of an experimental modified Arcan test under three load angles and a peel test were used to determine the 10 calibration parameters of the model. The obtained results show a good agreement between experimental and simulation results. It is advised to include peel test data to improve the accuracy of the equivalent model for SPR joints. The coupon level results show a good accuracy of the equivalent model, however, further validation in larger structures where interaction effects and more complex load conditions occur should be investigated. Weyer et al. [8] proposed another model for crash simulation of SPR joined structures. The model consists of a fastener element provided in the Abaqus code, which is calibrated using the experimental results of the modified Arcan and peel test of a SPR sample. The obtained model provided a sufficient accuracy, however the input of modified Arcan and peel test data is mandatory. Grujicic et al. [9] extended this methodology by using virtual experiments of a full scale SPR model to calibrate the simplified element. This approach can provide an advantage for designers with limited access to experimental facilities. Bérot et al. [10] developed an universal equivalent model which was calibrated using 6 experimental test cases all inducing different load cases onto the joint. The calibration parameters were obtained by a computational zero-order minimisation algorithm. Although good agreement with the simulation results was obtained for SPR joints, additional validation is needed to use it for other joining techniques. In this regard, the possibilities for clinched joints in this field have not been thoroughly investigated. Breda et al. [11] proposed an equivalent modelling strategy for a single clinched joint. It was shown that the latter approach enables to accurately reproduce the force-displacement behaviour under

quasi-static mixed mode loading for a single joint. Breda et al. [12] validated this equivalent clinch methodology for multi-joint configurations on lab coupon scale experiments and as well on a full-scale industrial test case involving a complex load distribution. The global response could be accurately reproduced by the proposed equivalent model.

In the majority of the cited work on equivalent modelling, experimental results are used to calibrate the governing parameters of the equivalent model. During these benchmark experiments, the base material is often plastically deformed and contains a residual material state due to forming operations prior to the joining of the test specimen. This paper scrutinizes two specific aspects systematically ignored in previous studies on the calibration of equivalent models for mechanical joints: i) the effect of residual stresses due to manufacturing of the test specimen ii) the effect of plastic anisotropy of the steel sheet itself, in the remainder of this referred to as base material. The former might affect the elastic calibration while the latter could potentially bias the calibration of the post-yield behaviour. The most important point here is that the experimental and computational effort associated with the calibration procedure depends on the complexity of the FE model. Indeed, the need for detailed material modelling and incorporation of residual stresses would increase the calibration effort of the equivalent model. This paper aims at clarifying the role of plastic anisotropy and residual stresses on the calibration procedure presented by Breda et al. [11] to arrive at a generic equivalent modelling strategy for clinched connections. Moreover, the intention is to enable extension of the research to other equivalent joint strategies following a similar approach. To this end, benchmark experiments (U-shear lap test and H-tension test) were conducted on low carbon steel. Coppieters et al. [13] performed extended experiments to characterize the low carbon steel presented in this paper with special attention to the plastic anisotropic of the material. The calibration procedure of the equivalent model is briefly summarized in section 2. In section 3, the characterization of the base material is discussed along with the benchmark experiments for cal-

ibration purposes. Section 4 gives an overview of all calibration models used with the results presented in section 5.

2. Equivalent model calibration procedure

Breda et al. [11] presented the calibration process and methodology for the equivalent clinch model. The key points of the calibration procedure, required for understanding the remainder of this paper, are briefly summarized in this section. The equivalent modelling strategy for clinched joints consists out of two main steps (Fig. 1). In a first step, two benchmark experiments are performed to capture the behaviour of the joint under different load conditions. A H-tension experiment is performed to capture the axial or pull-out behaviour of the joint while a shear lap experiment is used to capture the shear behaviour of the joint. During these experiments, the base material and joint behaviour contribute to the global force-displacement response of each specimen. In a second step, the global behaviour of the benchmark experiments is reproduced by a numerical procedure where the physical joint is replaced by an equivalent model. During the calibration procedure the local behaviour of the initially rigid equivalent model is softened elastically and plastically, until the global behaviour matches the experimental benchmark experimental results. In this way, the equivalent joint model is calibrated and can be used for multi-joint applications [12].

Given the scope of this paper, it is important to understand the mechanical representation of the equivalent joint model and the implementation of the local mechanical behaviour. The model consists of 2 elements (Fig.2): a connector with 6 degrees of freedom (d.o.f.) and a kinematic coupling which couples the connector end nodes to the sheet elements. All 6 d.o.f. of the connector enable to introduce elastic and plastic properties. The rotational d.o.f. around the local radial x and y axis are assumed to be fully rigid and the rotation around the axial direction z as free because of the physical mechanical properties of the clinch [11]. The mechanical behaviour of the 3 remaining translational d.o.f. is

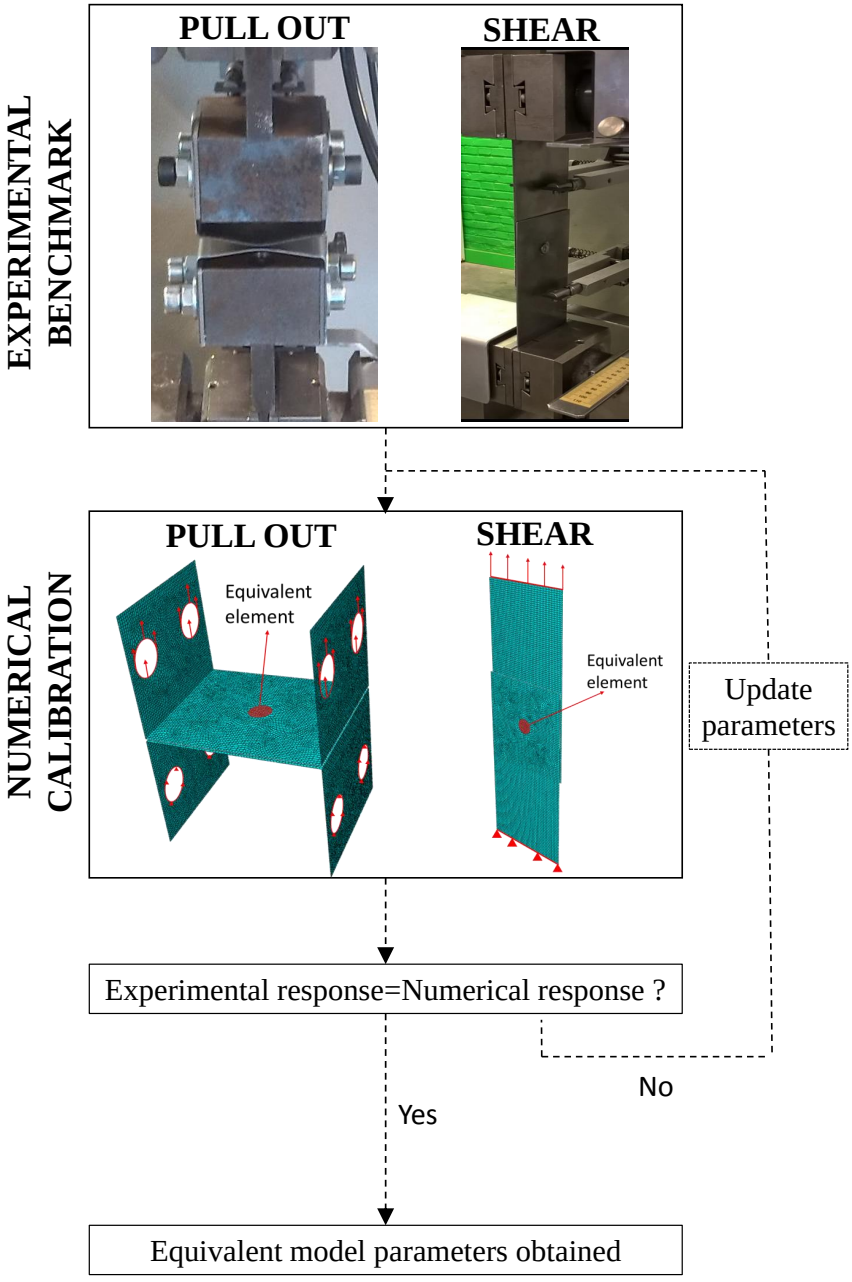

Figure 1: Equivalent modelling procedure

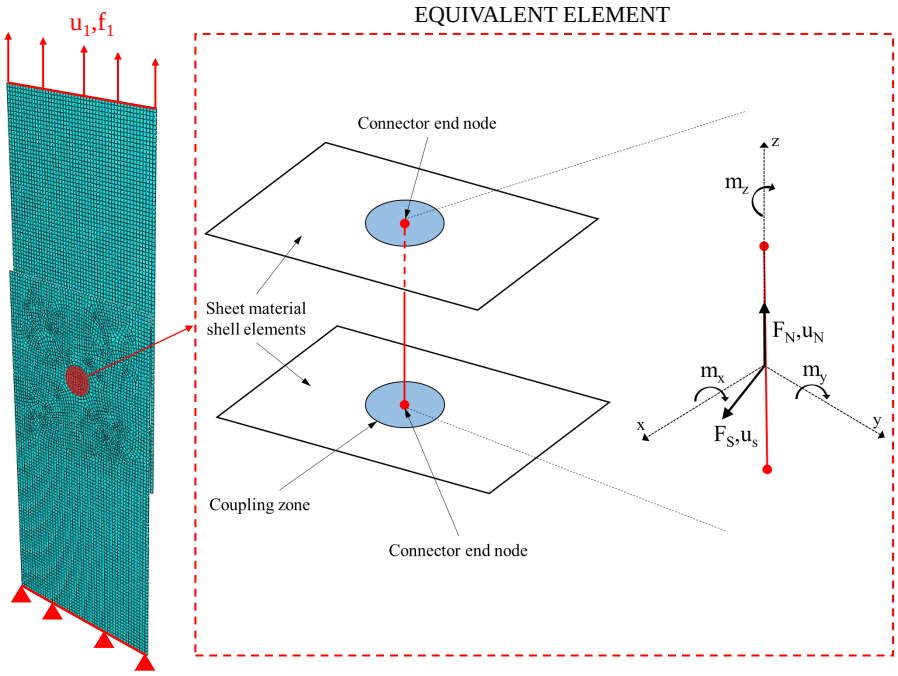

Figure 2: Equivalent model representation

calibrated using the numerical calibration procedure. For the considered joints in this paper, the radial behaviour, according to the x and y axis, can be assumed identical because of the axi-symmetrical nature of the joint. In the remainder of this paper this will be referred to as the shear behaviour (F_S,u_s) of the joint model. The translational behaviour according to the z-axis is referred to as the axial or normal behaviour of the joint model (F_N,u_N).

Fig. 3 shows a schematic representation of the calibration process to calibrate the shear behaviour of the connector. The approach to calibrate the normal direction of the joint is identical.

During the calibration process, the experimental force-displacement results of two benchmark experiments (shear lap and H-tension test) are compared with the global results (f_1,u_1 and f_3,u_3) of numerical models of these experiments containing the equivalent model for the clinch joint. The global force-displacement response of the numerical model can be seen as a combination of two non-linear

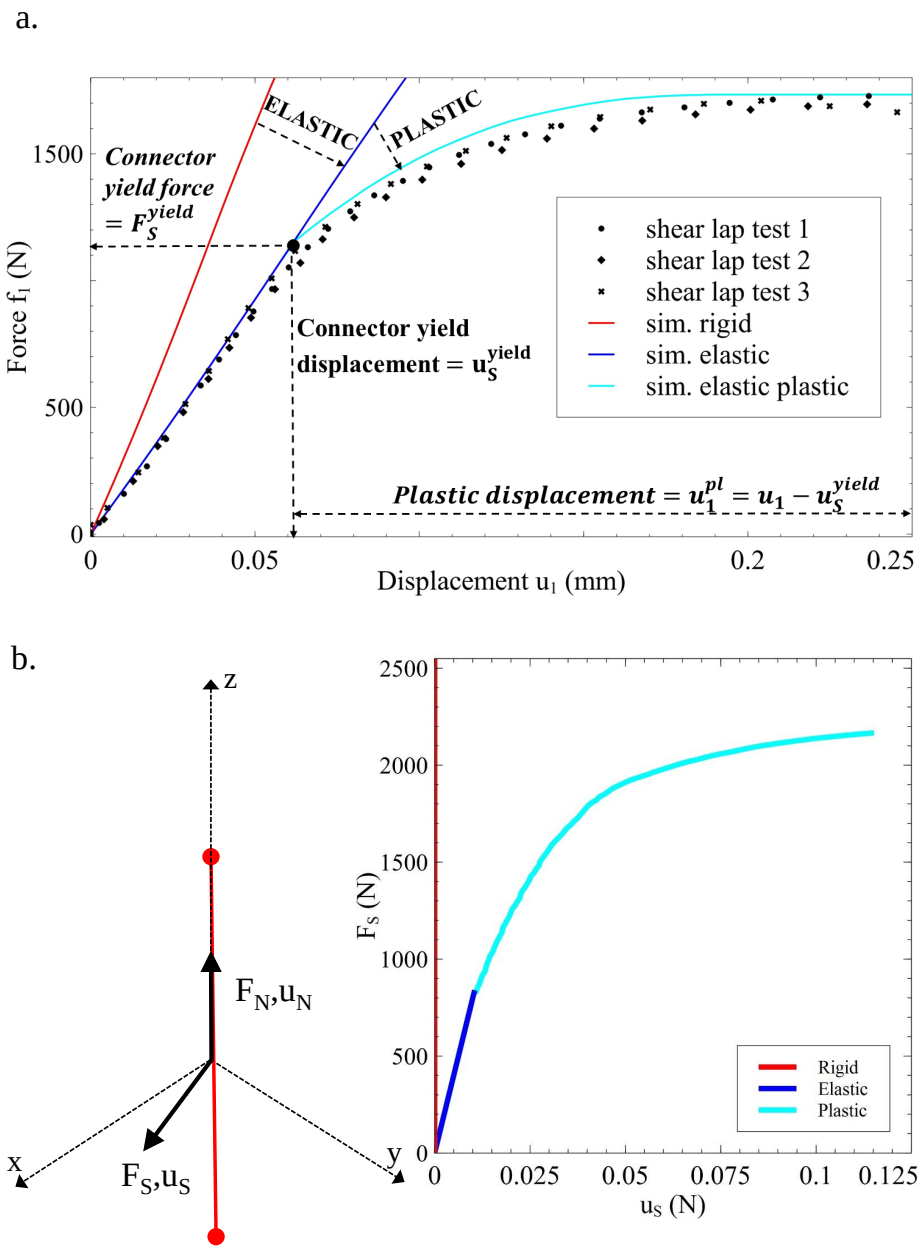

Figure 3: Plastic calibration step (shear direction): a. Global response b. Local connector response

springs. One will be the non-linear (elastic-plastic) response of the base material and the other is the non-linear (elastic-plastic) response of the equivalent model (F_N,u_N and F_S,u_S) which is initially assumed to be rigid. During the calibration process, the parameters of the equivalent model are softened in two steps until the global response of the spring system matches the experimental results. Firstly, the elastic stiffness D_S and D_N are determined for each load direction. Secondly, a connector yield force (F^{yield}) and the uncoupled plastic equivalent hardening laws for the connector are obtained. F^{yield} is determined by comparing the force values at fixed displacement values of the elastic simulation results with the experimental test results. The yield point of the connector (F^{yield},u^{yield}) is considered at the point at which divergence of the numerical elastic response with the experimental results occurs ($f^{sim.}$-$f^{exp.} \geq 10N$). With the yield point determined, the experimental global plastic relation between the force (f_1 and f_3) and plastic displacement (u_1^{pl} and u_2^{pl}) can be obtained as can be seen in Fig. 3. To transform this global behaviour to the local connector hardening behaviour (F_S,u_S^{pl} and F_N,u_N^{pl}) two scaling factors $K_{u,S}$ and $K_{u,N}$ are determined for each of the load directions using following equations 1 and 2.

For the shear direction:

$$F_S = \begin{cases} D_S \cdot u_S & if \quad F_S < F_S^{yield} \\ f(u_S^{pl}) = f(u_1^{pl} \cdot K_{u,S}) & if \quad F_S > F_S^{yield} \end{cases} \tag{1}$$

For the normal or axial direction:

$$F_N = \begin{cases} D_N \cdot u_N & if \quad F_N < F_N^{yield} \\ f(u_N^{pl}) = f(u_3^{pl} \cdot K_{u,N}) & if \quad F_N > F_S^{yield} \end{cases} \tag{2}$$

These scaling factors alter the hardening rate of the connector element for each load direction as can be seen in Fig.4. Convergence is reached as soon as the model experimental maximum load point equals the numerical maximum load point with sufficient accuracy.

In this way, the 6 parameters (D_S, D_N, F_S^{yield}, F_N^{yield},$K_{u,S}$ and $K_{u,N}$) for

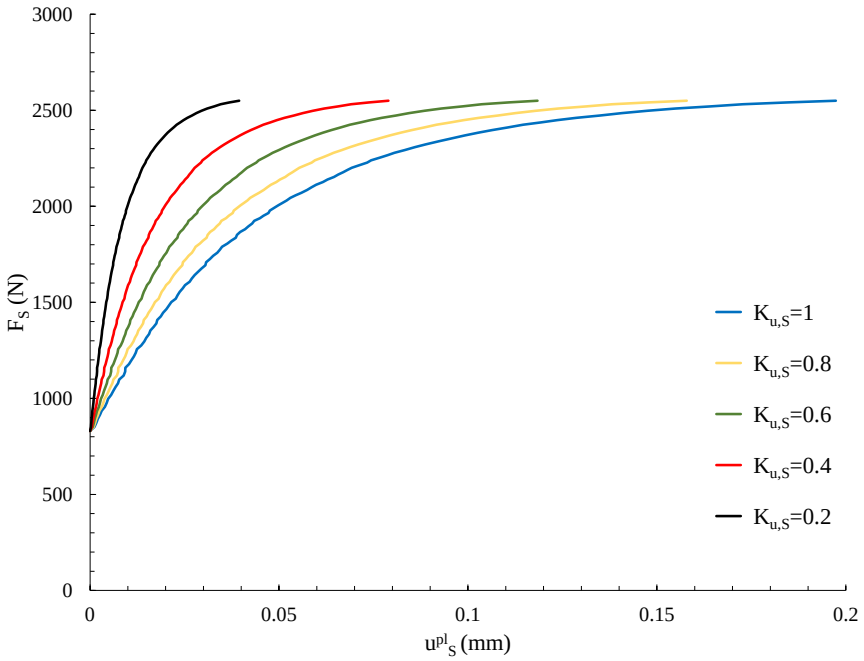

Figure 4: Shear connector behaviour for altering K-factor

the equivalent clinch model are obtained. The calibration routine merely minimizes the discrepancy between experimental and computed global response by modifying the parameters of the equivalent joint model. To do so, it relies on a FE model which incorporates a plane stress yield criterion assigned to the base material which might be subjected to large plastic deformations. Additionally, assumptions with respect to the boundary conditions have to be made. In case of a H-type tension test, the bending operation for manufacturing the test specimen can be included or ignored. These modelling choices might have an effect on the identified parameters of the equivalent model.

3. Material identification and joint properties

3.1. Material identification

As the plastic deformation of the base material during the benchmark experiments potentially affects the calibration procedure, an accurate characterisation of the base material is essential. A deep-drawing-quality steel sheet was chosen as base material in this study. The steel sheet has a nominal thickness of 1.2 mm. Standard tensile tests were conducted to determine the work hardening properties, the maximum uniform strain ϵ_{max} and the r-values under 0°, 45°, and 90° with respect to the rolling direction (RD). The values can be found in Table 1. The test material was assumed to be elastically isotropic (average measured Young's modulus = 233 GPa) and plastically orthotropic. Coppieters et al. [13] characterized the plastic anisotropy of the test material. To this end, the material was subjected to 7 linear stress paths in the first quadrant of the stress space using two types of biaxial tensile tests. Kuwabara et al. [14] presented the biaxial tensile test to measure differential work hardening of steel sheet. Later, Kuwabara et al. [15] presented the multi-axial tube expansion test to measure this behaviour of steel sheet for large plastic deformations. Both experiments were adopted to obtain the plastic material behaviour under multi-axial load conditions of the base material used in this paper. Coppieters et al. [13] concluded that the shape of the yield locus for this steel remains constant as from

Table 1: Swift's hardening law $\left(\sigma = K(\epsilon_0 + \epsilon_{eq}^{pl})^n\right)$ fitted in a strain range from $\epsilon_{eq}^{pl} = 0.002$ up to the maximum uniform strain ϵ_{max} . The reported r-values are the measured values at an engineering strain ϵ_{eng}=0.10 using gauge marks.

Tensile direction	$\sigma_{0.2}$ (MPa)	K (MPa)	ϵ_0	n	r	ϵ_{max}
RD (x)	153	564	0.0059	0.275	1.85	0.248
45°	161	558	0.0072	0.272	1.93	0.254
90° (y)	162	549	0.0080	0.272	2.82	0.259

Table 2: Calibrated Yld2000-2d parameters at a reference plastic strain ϵ_0^p=0.24.

α_1	α_2	α_3	α_4	α_5	α_6	α_7	α_8	M
0.9394	1.1841	0.8872	0.8765	0.9333	0.8020	1.0462	1.0227	5.90

$\epsilon_{0,ref}^p$=0.03. Beyond that value, the plastic work contours are homothetic and isotropic hardening is valid. Consequently, the yield function can be calibrated at an arbitrary reference plastic strain in the range 0.03< $\epsilon_{0,ref}^p$ ≤0.24. The experimental data obtained by Coppieters et al. [13] was used to calibrate three selected plane stress yield functions: the von Mises [16] criterion, the Hill'48-r [17] criterion and the Yld2000-2d anisotropic yield function [18]. Swift's strain hardening law (Table 1) was used to describe the reference strain hardening in the RD of the test material. The plane stress version of Hill's 48 yield criterion was calibrated by using the r-values reported in Table 1. The anisotropic parameters α_i (i=1-8) of the Yld2000-2d yield function (Table 2) were calibrated for a reference plastic strain $\epsilon_{0,ref}^p$ equal to the maximum uniform strain, i.e. $\epsilon_{0,ref}^p$=0.24. The calibrated normalised yield loci are shown in Fig. 5. Coppieters et al. [13] found that the Yld2000-2d yield function, as opposed to the von Mises and the r-based Hill48 yield criterion, could accurately reproduce the experimental data beyond a reference plastic strain of $\epsilon_{0,ref}^p$=0.03.

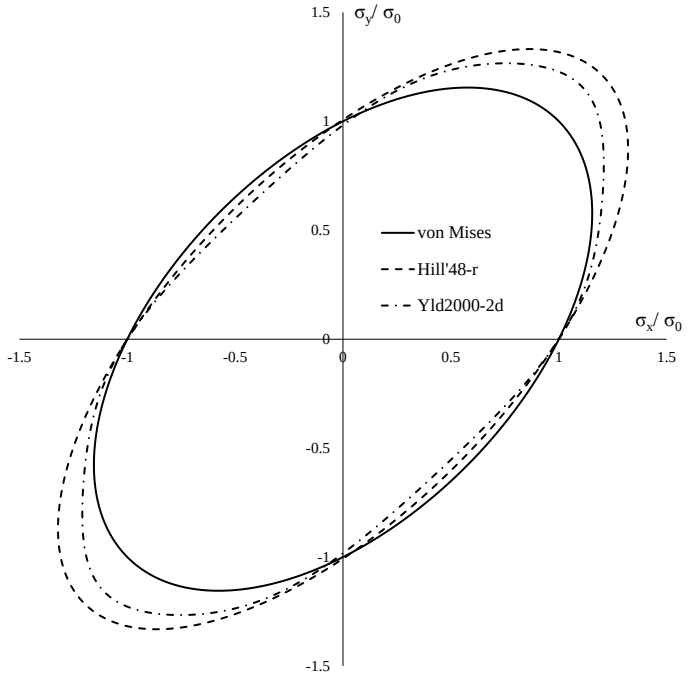

Figure 5: Selected yield functions normalized by σ_0. The rolling direction is aligned with the X-axis.

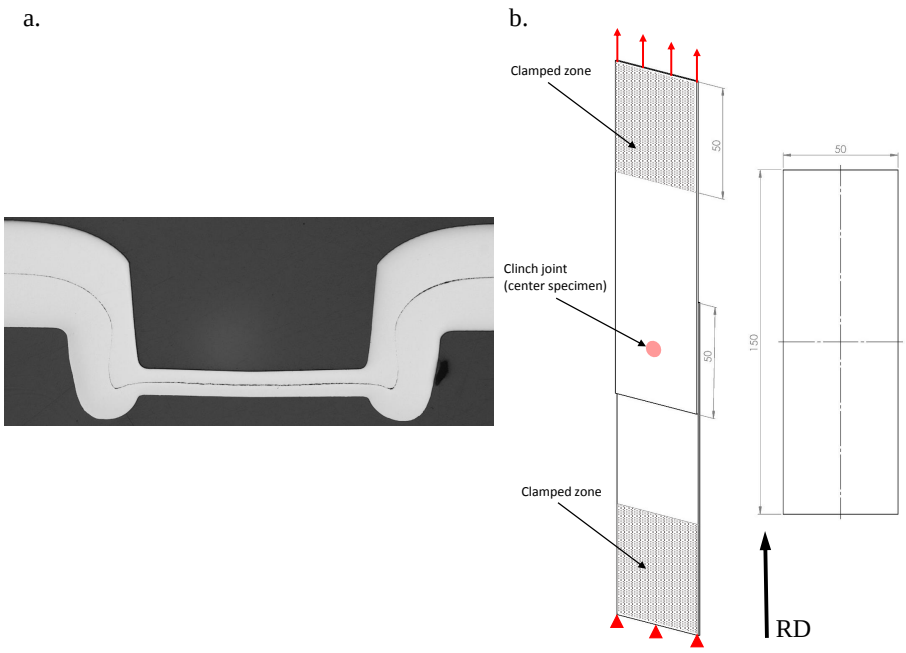

Figure 6: a. Clinch joint section b. Shear lap specimen geometry with rolling direction (RD)

3.2. Joint properties

All specimens in this paper were joined using the non-cutting single stroke clinch (NCSS) technique using a closed die with a diameter of 8 mm. The large ductility of the low-carbon steel enables to produce a defect-free clinched joint as shown in Fig. 6 a. The diameter of the punch was 5 mm resulting in a joint bottom thickness of 0.55 mm which creates an optimal interlock for the used base material. The experimental joint properties for this work were determined using two benchmark experiments (shear lap test and H-tension test). All experiments were performed using a standard tensile machine with a capacity of 10kN and a cross-head speed of 1 mm/min. All specimens were fabricated using water jet cutting.

3.2.1. Shear lap experiments

To obtain the shear behaviour of the joint, a shear lap test was conducted as originally proposed in [11]. An extensometer was used to measure the elongation of the specimen. The geometry of this specimen can be found in Fig. 6 b. The results can be found in Fig. 7 a. During the experiment, plastic asymmetrical secondary bending could be observed during the experiment (Fig. 8). This effect results in rotation of the joint during loading which introduces a normal load in the joint during the test and eventually leads to unbuttoning of the joint. As soon as the secondary bending occurs, the pure shear load condition in the joint is no longer valid as a normal component will be introduced. To avoid this, and capture the pure shear properties of the joint, an alternative experiment using U-shear specimen (Fig. 9) was performed. The U-shape of the specimen stiffens the base material which avoids secondary bending during the experiment. DIC was used to capture the elongation during the experiment (Fig.10). The results of the U-shear test can be found in Fig. 11. The results of *U-shear 3* can be considered as an outlier and is discarded. The response of *U-shear 2* was used to calibrate the model parameters.

3.2.2. Pull-out experiments

A H-tension test as proposed in [11] was used as benchmark experiment to obtain the normal joint response for the calibration procedure. The H-tension specimen, which consists of 2 U-shaped specimen (Fig. 12) folded prior to the clinching process, was mounted in a fixture which is clamped inside a tensile machine (Fig. 13 b.). The displacement of the fixture was captured using an extensometer. The results of the experiment, can be found in Fig. 13 a. The results of *H-tension 1* were used to calibrate the equivalent model.

4. Numerical models

The FE models used in the calibration procedure uses a 4-node shell element with reduced integration (S4R). All analyses are executed using the Abaqus/standard solver.

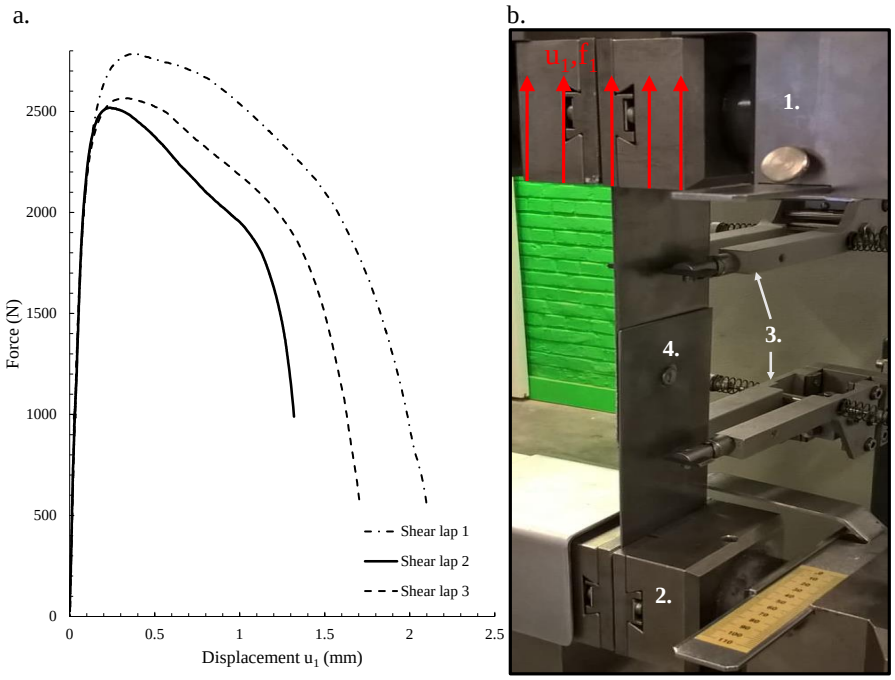

Figure 7: Shear lap experiment: a. Results b. Test set-up (1.Upper clamp 2.Lower clamp 3.Extensometer 4.Shear lap specimen 5.Fixture)

Figure 8: Secondary bending

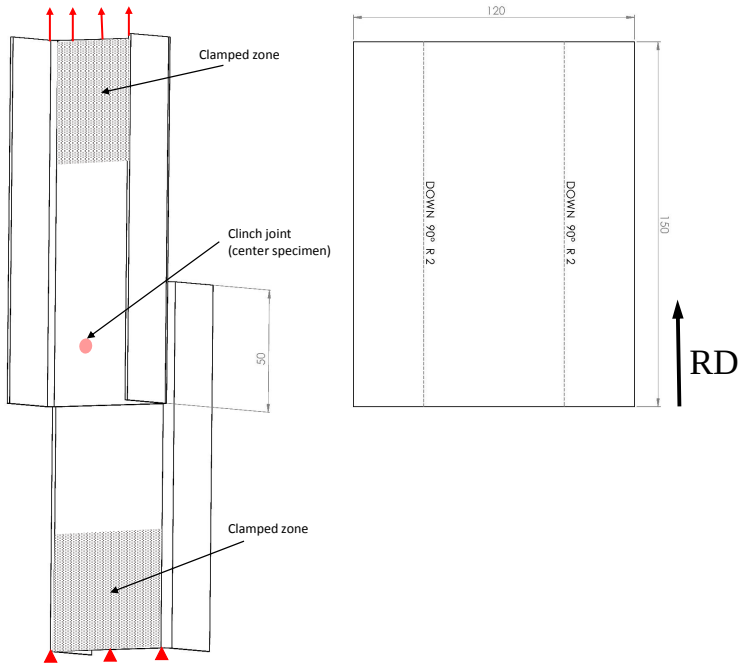

Figure 9: U-shear lap specimen geometry with rolling direction (RD)

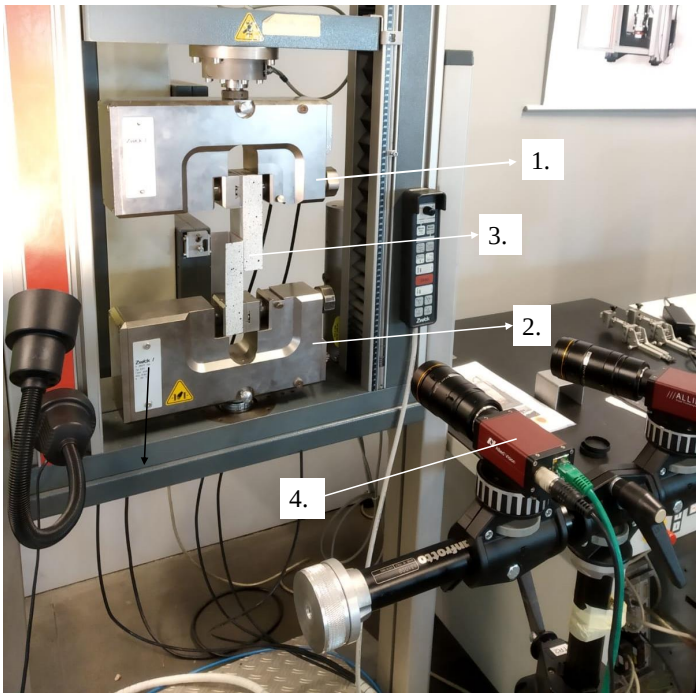

Figure 10: U-shear lap experiment set-up: 1.Upper clamp 2.Lower clamp 3.U-shear specimen 4.Camera set-up

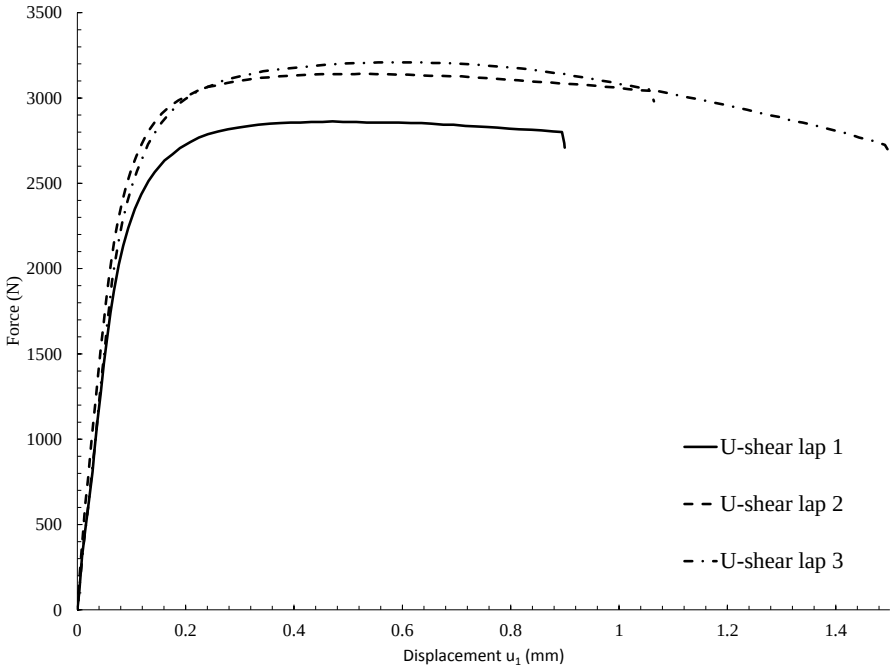

Figure 11: U-shear lap test results

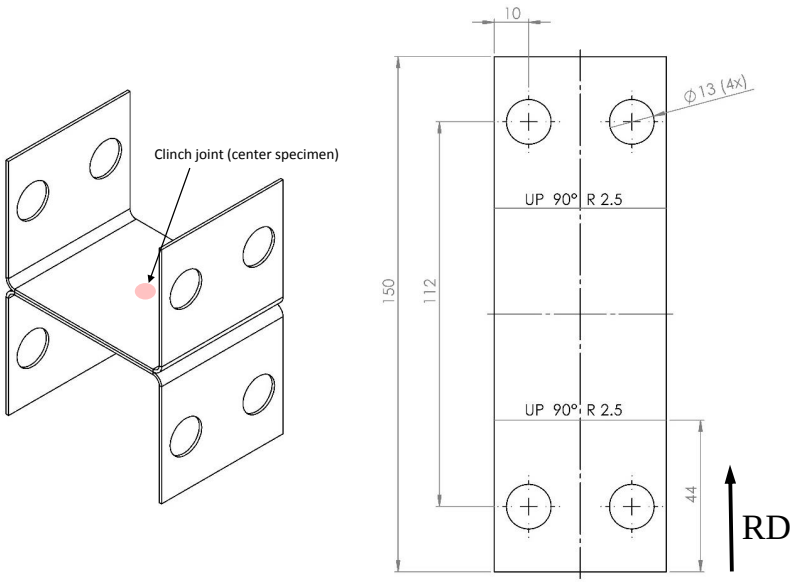

Figure 12: H-tension specimen geometry with rolling direction (RD)

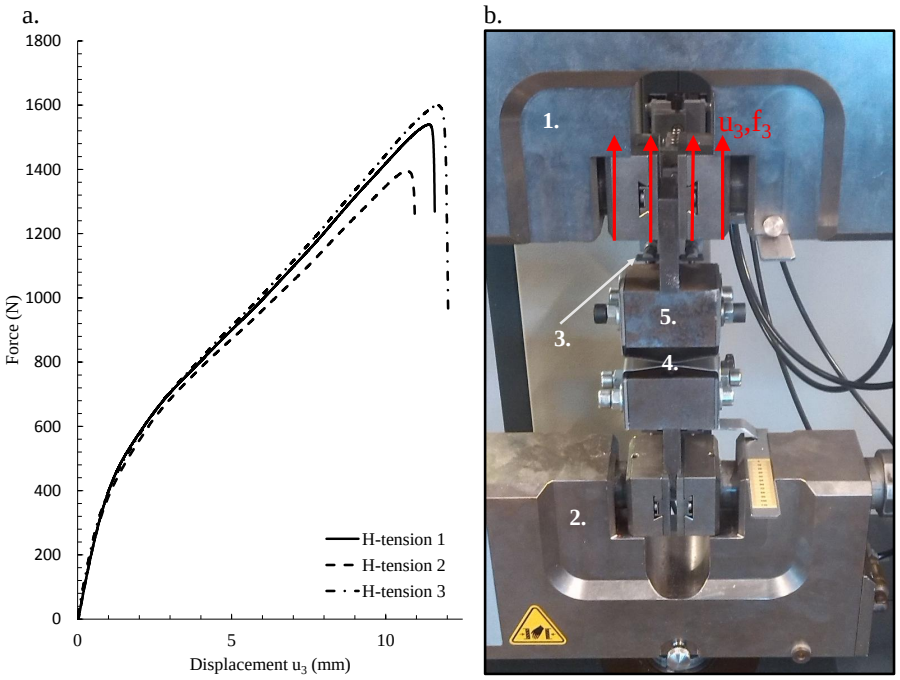

Figure 13: H-tension experiment: a. Results b. Test set-up

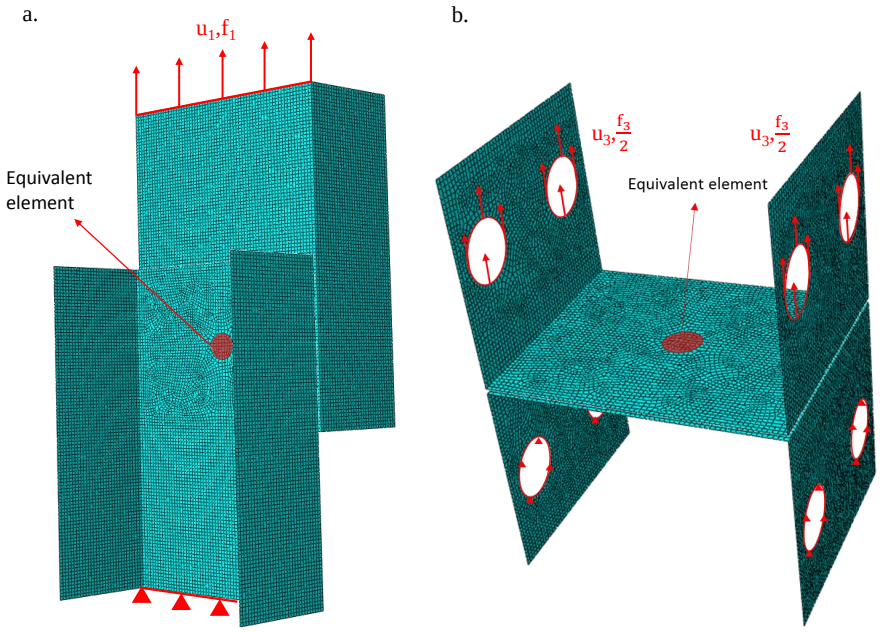

Figure 14: Numerical calibration models: a. U-shear model b. H-tension model

4.1. Shear

An overview of the shear calibration model can be found in Fig.14 a. In order to calibrate the shear behaviour, three selected yield functions were used to model the base material. The first model (*HS-1*) uses the von Mises yield criterion, assuming isotropic plasticity. The second (*HS-2*) and the third (*HS-3*) shear model adopt an anisotropic yield function, namely the Hill48-r yield function and the Yld2000-2d yield function, respectively. The parameters of the anisotropic yield functions can be found in section 3.1. These models were used to obtain the calibration parameters for the shear behaviour of the equivalent model as presented in section 2.

4.2. Pull-out

Breda et al. [11] initially proposed the H-tension test to calibrate the axial parameters for the equivalent model. The reduced doming effect during this

type of test results in a higher normal strength of the joint compared to alternative pull-out tests favoured the choice to be used as a reference test for calibrating the equivalent model. Although this method provided good results, the residual stresses in the material due to the bending process, required for manufacturing the H-type specimen prior to clinching, can affect the equivalent model parameters. In analogy with section 4.1, three different yield functions were used for calibrating the axial behaviour of the equivalent joint model. The folded geometry was initially applied for model set *PU-1*, *PU-2* and *PU-3*. For these models, the residual material state was ignored, and the virgin material state was applied prior to the calibration step.

A numerical simulation of the bending process was performed for models *PU-4*, *-5* and *-6*. As such, these models incorporate the residual stress state after bending the base material. This process consisted of 4 modelling steps which can be seen in Fig. 15: (a) first bending step and spring back, (b) second bending step and spring back, (c) re-orientation prior to equivalent model application, and (d) calibration step. As a result, a U-shaped specimen containing the residual stresses of the bending process was obtained.

A visualisation of the H-tension calibration models can be found in Fig. 14 b. As the specimen was mounted inside a clamping device, only the bolted regions were constrained during the simulation.

5. Results and discussion

The purpose of this work is to evaluate the effect of plastic anisotropy of the base material on the elastic and plastic calibration of an equivalent joint model for clinched connections. The main findings should help to improve the accuracy of equivalent modelling strategies. The results are discussed in this section for each load direction (shear and normal/axial).

5.1. Shear behaviour

The resulting shear calibration parameters for all yield functions can be found in Table 3. It can be seen that all the obtained calibration parameters

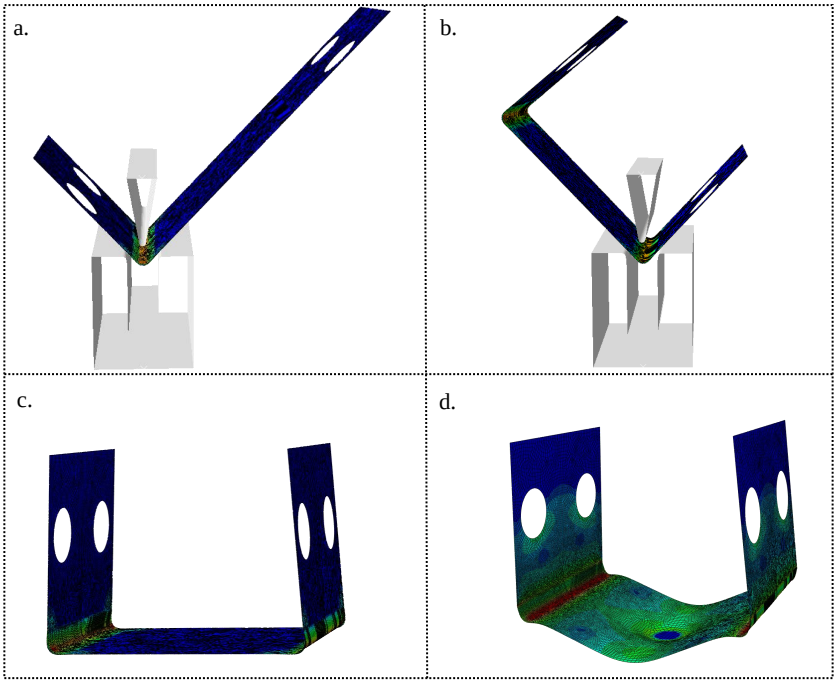

Figure 15: Simulation of the bending process prior to mechanical testing: a) First fold b) Second fold c) Reposition d) Calibration

Table 3: Calibration parameters shear lap test

Model	Radius (mm)	Yield function	D_S (N/mm)	F_S^{yield}(N)	$K_{u,S}$
HS-1	4	von Mises	80000	730	0.58
HS-2	4	Hill48-r	80000	730	0.58
HS-3	4	Yld2000-2d	80000	730	0.58

(elastic and plastic) are identical. For this type of joint, it can be concluded that the incorporation of an anisotropic yield function does not affect the elastic-plastic shear calibration parameters. The reason for this is twofold. Firstly, due to the folding of the sides, the U-shear specimen is stiffened which reduces plastic deformation of the base material confining the plastic deformation to the (proximity of the) clinched joint. Secondly, after elastic calibration of the equivalent model, the numerical response of the model is independent of the chosen yield function as can be observed in Fig. 16. At relatively high forces, very small deviations of the numerical elastic response start to occur due to plastification of the anisotropic base material. The latter observation occurs well above the maximum experimental force, hence irrelevant for the calibration process. Nevertheless, to limit the plastic deformation of the base material, it is recommended to use a U-shaped shear specimen for calibration purposes. In this way, anisotropy of the base material can be safely ignored when calibrating the shear behaviour of the equivalent joint model.

5.2. Normal or axial behaviour

The obtained normal or axial calibration parameters for each pull-out model are summarized in Table 4. Furthermore, the relative error for each resulting calibration parameters set, compared to the benchmark simulation *PU-6*, is shown. As opposed to the shear behaviour, it can be interfered that the plastic anisotropy of the base material affects the axial behaviour of the equivalent joint model. Firstly, it can be concluded that the residual material state has an effect on the obtained elastic stiffness calibration parameter while the adopted mate-

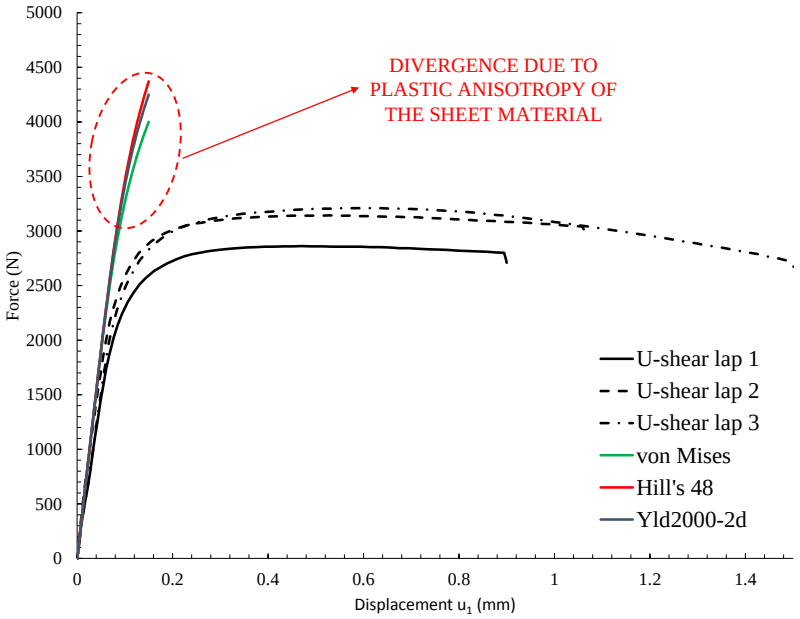

Figure 16: Numerical simulation response after elastic (shear) calibration

Table 4: Calibration parameters pull-out test with relative error

Model	Radius (mm)	Yield function	Initial material state	D_N (N/mm)	F_N^{yield}(N)	$K_{u,N}$
PU-1	4	von Mises	no	3400 (25.9%)	375 (38.4%)	0.035 (77.4%)
PU-2	4	Hill48-r	no	3400 (25.9%)	229 (15.5%)	0.11 (29%)
PU-3	4	Yld2000-2d	no	3400 (25.9%)	251 (7.4%)	0.08 (48.4%)
PU-4	4	von Mises	yes	2700 (0%)	465 (71.6%)	0.13 (16.1%)
PU-5	4	Hill48-r	yes	2700 (0%)	256 (5.5%)	0.18 (16.1%)
PU-6	4	Yld2000-2d	yes	2700 (reference value)	271 (reference value)	0.155 (reference value)

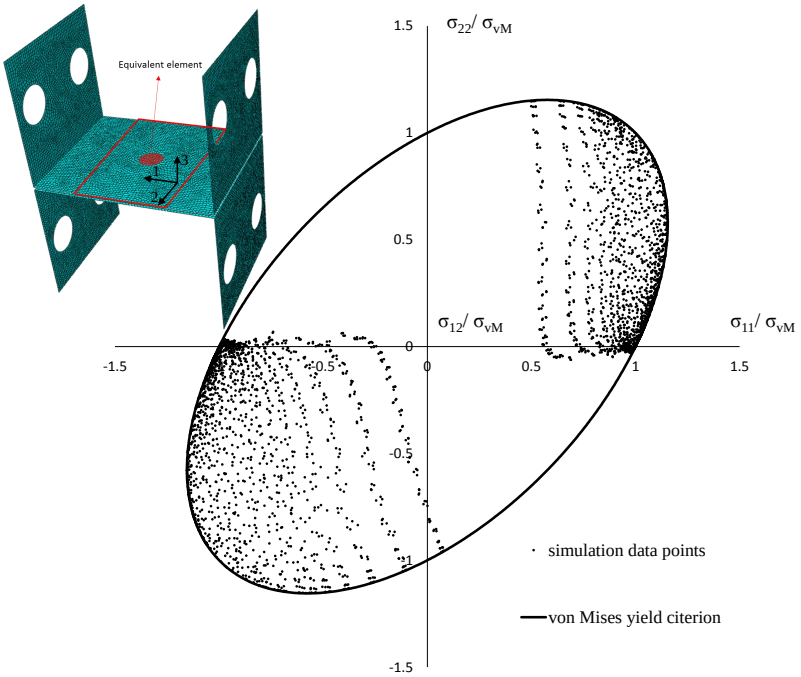

Figure 17: Normalised biaxial stress states in the upper sheet (red rectangular) during the H-tension simulation with rigid connector (maximum elongation). The von Mises criterion was adopted.

rial model has no significant influence on the obtained elastic stiffness calibration parameter D_N. Indeed, the local strain hardening due to the bending operation increases the stiffness of the H-specimen where the clinch joint is located during mechanical loading. Ignoring this effect during the elastic calibration will result in a substantial higher normal stiffness of the connector (25.9%). It must be noted that this error has a limited effect on the global force-displacement curve when probing a single joint. However, it is important to understand that this error accumulates when a large amount of equivalent models are present in a structure. In the latter case, it is recommended to account for the residual material state in the calibration procedure of the equivalent model.

In section 2 is shown that the plastic equivalent hardening law, which in-

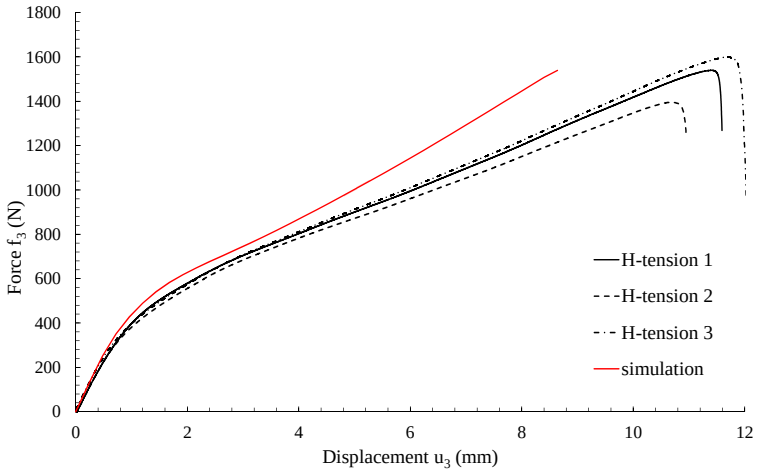

Figure 18: H-tension simulation using von Mises calibration parameters with accurate (Yld2000-2d) base material response.

cludes scaling factor $K_{u,N}$, is dependant of the determined connector yield point (F_N^{yield},u_N^{yield}). In turn, the connector yield point will affect the plastic calibration of the equivalent joint model. From Table 4 it can indeed be interfered that the plastic calibration parameters are influenced by the adopted yield function as well as the residual material state. The influence of the adopted yield function can be explained by the plastic deformation of the base material surrounding the equivalent model during the H-tension simulation prior to calibration. Fig. 17 shows the normalised stress states that occurs in the upper sheet during the initial H-tension simulation with a rigid connector. It can be seen that the surrounding base material is subjected to biaxial tension (lower sheet surface) and compression (upper sheet surface). Given the presence of these biaxial stress states associated with the plastification of the base material, the calibration accuracy of the plastic parameters of the equivalent model is determined by the accuracy of the adopted yield function. Indeed, the deficiency of the von Mises yield criterion for accurately modelling the plastic response of the base material, is compensated with a higher yield force of the connector and an increased hardening rate (i.e. a low $K_{u,N}$ value). This can be explained by the underestimation of the von Mises yield criterion to predict yielding in pure biaxial tension/compression of the anisotropic base material considered in this paper (Fig. 5). Assessment of the relative errors show that Hill's 48 yield criterion significantly improves the calibration accuracy of the equivalent joint model. The latter suggests that Hill's 48 yield function captures plastic yielding more accurately than the von Mises yield criterion. For a reference plastic strain of $\epsilon^p_{0,ref}$=0.24, it can indeed be inferred from Fig. 5 that Hill's 48 yield function is in better agreement with the reference Yld2000-2d yield function compared to the von Mises criterion.

The influence of the residual stress state on the plastic calibration is a result of the identified elastic stiffness. A lower axial connector elastic stiffness will lead to a higher yield force and lower axial scaling factor $K_{u,N}$ (i.e. a decreased hardening rate). To mitigate this effect, an alternative calibration sample such as a cross tension sample [11] is recommended to calibrate plastic equivalent

behaviour of the normal or axial direction of the joint.

The consequence for a design engineer ignoring plastic anisotropy and residual stresses during the calibration procedure, could lead to an over- or underestimation of the sheet deformation when applying the equivalent model for structural analysis. For the material studied in this paper, the von Mises criterion would not give acceptable calibration parameters for structural analysis and would result in relatively large errors. This is exemplified by Fig. 18 where the response of a H-tension experiment was predicted using: i) equivalent model parameters, calibrated using a von Mises calibration model (*PU-1*) ii) base material model accounting for the Yld2000-2D yield function with included residual material state (*PU-6*). The latter resulted in a global overestimation of the mechanical response by the numerical model. The findings discussed in this section are valid for conventional NCSS clinch joints applied to low carbon steel. Future work can focus on the effect of plastic anisotropy when novel clinch techniques are used, such as hole clinching [19, 20]. Furthermore, an upper bound for the degree of plastic anisotropy guaranteeing a reliable calibration of the equivalent model or introducing a correction factor to include the effect of residual stresses can be investigated in future work.

6. Conclusion

To improve the simulation accuracy of an equivalent clinch model, the effect of plastic anisotropy of the base material on the calibration procedure of the equivalent model was investigated. Two benchmark experiments were used to calibrate an equivalent clinch model. A H-tension test was applied to obtain the axial or normal parameters of the model. A U-shear lap specimen was adopted to obtain the pure shear behaviour of the joint by avoiding secondary bending of the steel sheet. The effect of the adopted anisotropic yield function and the relevance of considering the residual material state on the calibration accuracy of the equivalent model was scrutinized. Following conclusions are drawn for

the base material used in this paper:

1) In order to avoid secondary bending, a U-shear specimen can be applied to obtain the pure shear properties of the joint. During the calibration process, potential plastic anisotropy can be ignored to obtain an accurate shear behaviour of the equivalent joint model. The von Mises yield function can be safely used to obtain accurate shear parameters of the equivalent model thereby reducing the experimental effort associated with the calibration of the equivalent model.

2) The residual material state has a direct effect on the calibration of the axial stiffness parameters and an indirect effect on the determination of the connector plastic yield point. Accurate calibration of the axial plastic behaviour of the equivalent joint model requires to consider plastic anisotropy. The selection of the anisotropic yield function affects the accuracy of the determined yield point and scaling factor due to biaxial stress states which occur in the proximity of the equivalent model during the axial calibration procedure. Ignoring plastic anisotropy can lead to inaccurate axial calibration parameters and large errors. This can result in over- or underestimating the sheet deformation in a clinch assembly.

Both findings can help design engineers to improve the accuracy of current and future equivalent models. In this way, the prediction of the mechanical response for structures containing a large number of joints can be improved.

References

References

[1] B. Langrand, E. Deletombe, E. Markiewicz, P. Drazétic, Riveted joint modeling for numerical analysis of airframe crashworthiness, Finite Elements

in Analysis and Design 38 (2001) 21–44.

[2] R. Porcaro, A. G. Hanssen, A. Aalberg, M. Langseth, Joining of aluminium using self-piercing riveting: Testing, modelling and analysis, International Journal of Crashworthiness 9 (2) (2004) 141–154.

[3] S. Coppieters, P. Lava, R. Van Hecke, S. Cooreman, H. Sol, P. Van Houtte, D. Debruyne, Numerical and experimental study of the multi-axial quasi-static strength of clinched connections, International Journal of Material Forming 6 (2013) 437–451.

[4] S. Xu, X. Deng, An evaluation of simplified finite element models for spot-welded joints, Finite Elements in Analysis and Design 40 (2004) 1175–1194.

[5] N. Khandoker, M. Takla, Tensile strength and failure simulation of simplified spot weld models, Materials and Design 54 (2014) 323–330.

[6] M. Palmonella, M. I. Friswell, J. E. Mottershead, A. W. Lees, Finite element models of spot welds in structural dynamics: review and updating, Computers and Structures 83 (2005) 648–661.

[7] A. G. Hanssen, L. Olovsson, R. Porcaro, M. Langseth, A large-scale finite element point-connector model for self-piercing rivet connections, European Journal of Mechanics - A/Solids 29 (2010) 484–495.

[8] S. Weyer, H. Hooputra, F. Zhou, Modeling of self-piercing rivets using fasteners in crash analysis, in: 2006 ABAQUS Users' Conference, 2006.

[9] M. Grujicic, J. Snipes, S. Ramaswami, F. Abu-Farha, Self-piercing riveting process and joint modeling and simulations, SAS 3 (2014) 20–29.

[10] M. Bérot, J. Malrieu, F. Bay, An innovative strategy to create equivalent elements for modelling assembly points in joined structures, Eng. Computation. 31 (2014) 453–466.

[11] A. Breda, S. Coppieters, D. Debruyne, Equivalent modelling strategy for a clinched joint using a simple calibration method, Thin Walled Structures 113 (2017) 1–12.

[12] A. Breda, S. Coppieters, A. V. de Velde, D. Debruyne, Experimental validation of an equivalent modelling strategy for clinch configurations, Materials & Design 157 (2018) 377 – 393.

[13] S. Coppieters, T. Hakoyama, P. Eyckens, H. Nakano, A. Van Bael, D. Debruyne, T. Kuwabara, On the synergy between physical and virtual sheet metal testing: calibration of anisotropic yield functions using a microstructure-based plasticity model, International Journal of Material Forming (2018) 1–19.

[14] T. Kuwabara, S. Ikeda, T. Kuroda, Measurement and analysis of differential work hardening in cold-rolled steel sheet under biaxial tension, J. Material Process. Technol. 80/81 (1998) 517–523.

[15] T. Kuwabara, F. Sugawara, Multiaxial tube expansion test method for measurement of sheet metal deformation behavior under biaxial tension for a large strain range, Int. J. Plast. 45 (2013) 103–118.

[16] R. Von Mises, Mechanik der festen Korper un plastich deformablen Zustant. Gottingen Nachrichten, Math. Phys. Kl., 1913.

[17] R. Hill, A theory of the yielding and plastic flow of anisotropic metals, Proc. R. Soc. Lond. A193 (1033) (1948) 281–297.

[18] F. Barlat, J. Brem, J. Yoon, K. Chung, R. Dick, D. Lege, F. Pourboghrat, S.-H. Choi, E. Chu, Plane stress yield function for aluminum alloy sheets—part 1: theory, International Journal of Plasticity 19 (9) (2003) 1297 – 1319.

[19] S.-H. Lee, C.-J. Lee, K.-H. Lee, J.-M. Lee, B.-M. Kim, D.-C. Ko, Influence of tool shape on hole clinching for carbon fiber-reinforced plastic and sprc440, Advances in Mechanical Engineering 6 (2014) 1–12.

[20] C.-J. Lee, J.-M. Lee, H.-Y. Ryu, K.-H. Lee, B.-M. Kim, D.-C. Ko, Design of hole-clinching process for joining of dissimilar materials – al6061-t4 alloy with dp780 steel, hot-pressed 22mnb5 steel, and carbon fiber reinforced plastic, Journal of Materials Processing Technology 214 (2014) 2169 – 2178.